PROCEEDINGS OF SCIENCE

New 3D models of interstellar gas and their impact on high-energy interstellar emission

Guðlaugur Jóhannesson*
Science Institute, University of Iceland, IS-107 Reykjavik, Iceland
AlbaNova Univ. Center Nordita, Roslagstullsbacken 23, SE-106 91 Stockholm, Sweden
E-mail: gudlaugu@gmail.com

Troy Porter
W. W. Hansen Experimental Physics Laboratory and Kavli Institute for Particle Astrophysics and Cosmology, Stanford University, Stanford, CA 94305, USA
E-mail: tporter@stanford.edu

Igor Moskalenko
W. W. Hansen Experimental Physics Laboratory and Kavli Institute for Particle Astrophysics and Cosmology, Stanford University, Stanford, CA 94305, USA
E-mail: imos@stanford.edu

The interstellar gas plays a key role in the astrophysics of cosmic-rays (CRs). The gas serves as a target for the CR particles causing energy losses and generation of secondary CR particles and the high-energy interstellar emission. Observations of the spectra and abundances of these secondary particles are used to decipher the propagation history of CRs and to decode possible signatures of new physics. Until now, most calculations of CR propagation have used 2D cylindrically symmetric models for the distribution of the interstellar gas. This is partly due to the inevitable difficulties in determination of the 3D gas distributions. We present a method for determination of the 3D distribution of interstellar gas and our preliminary results. We discuss the effect these new 3D models may have on the analysis and interpretation of CR propagation and high-energy interstellar emissions.

7th Fermi Symposium 2017
15-20 October 2017
Garmisch-Partenkirchen, Germany

*Speaker.

1 Introduction

The interstellar emission resulting from cosmic rays (CRs) interacting with the interstellar medium (ISM) in the Galaxy is a prominent feature of the γ-ray sky and is responsible for more than half of the photons observed by the *Fermi*–LAT. Most of the current interstellar emission models (IEMs) assume a 2D cylindrically symmetric distribution of CRs [1, 2]. While they provide a reasonable fit to the *Fermi*–LAT data, residuals of the order of few tens of percent are visible on scales ranging from a few to tens of degrees. Some of those are likely related to large scale structures in the CR and ISM that is not encapsulated in the 2D models. These new data have inspired progress towards a more detailed 3D models for the high energy interstellar emission [3, 4, 5]. This work follows a similar path focusing on the distribution of interstellar gas and how its distribution affects the expected distribution of CRs.

Knowledge of the distribution of interstellar gas comes mostly from observation of the H I 21-cm line and CO 2.6-mm line [6]. The line emission strength is related to the column density of interstellar gas and under assumptions of cylindrical gas motion the Doppler shift of the emission lines can be used to infer the distance to the emitting gas. This gives a direct mapping from the observed line emission (l, b, v) to the density of interstellar gas (x, y, z) [7, 8, 9]. This mapping is however not without issues. Thermal and turbulent motions of the gas create a spread in the Doppler shift that directly relates back to spread in distance estimates resulting in elongated features along lines of sight. The gas is also not in a purely cylindrical motion around the Galactic centre (GC) and those non-cylindrical velocities dominate the Doppler shift along directions towards and away from the GC resulting in regions with no distance information. In this work we instead use the inverse mapping $(x, y, z) \rightarrow (l, b, v)$ and parameterise the gas density distribution. The parameters are adjusted in a maximum likelihood fit to the emission line data. This enforces continuity across directions were non-cylindrical motions dominate and reduces the effect of random gas motion because smoothing is applied to the model. This comes at the expense of fine structure in the model that is difficult to account for unless the number of parameters in the model becomes unreasonably large.

2 3D modeling of the interstellar gas

The parameters of the model are optimised using a maximum-likelihood fit to the H I LAB survey [10] and the DHT CO survey [11]. The survey data is re-binned to a HEALPix grid [12] using HEALPix order 7 for H I while order 8 is used for the CO data. The spatial resolution is chosen to resolve the latitudinal dependence of the gas distribution toward the GC. The velocity resolution of both surveys is degraded to 2 km s^{-1}, which is smaller than the expected line broadening due to turbulent and thermal emotion that is assumed to be 6 km/s and 10 km/s for CO and H I respectively. The statistical uncertainty on the data is assumed to be constant over the entire sky and values of 0.05 K for CO and 0.1 K for HI are assumed, which are in agreement with the noise estimate for the original surveys taking into account the re-binning. Even though the noise in the surveys is normally distributed, a student-t likelihood is used to reduce sensitivities to large outliers that are inevitable because the model cannot capture the finest structures in the line emission observations.

The model consists of two parts, the density of the gas $n_x(\vec{X})$ and the velocity field of the gas $\vec{v}(\vec{X})$, where $\vec{X}$ is the position in the Galaxy and the subscript x can be either H I or CO. For each line-of-sight the velocity field is used to calculate the expected Doppler shift as a function of distance to set the integration boundaries of the model. The density is then integrated along the line-of-sight and converted to line intensity. For H I the radiative transport equation is used to estimate the line intensity assuming the gas is optically thin. For CO the line intensity is assumed linearly related to the density, which is suitable if the final model is turned into H_2 densities using the X_{CO} factor.

For this contribution we use a simple geometrical models for the density and cylindrical rotation using the rotation curve from [13]. Because the model does not provide any distance information around the GC and anti-centre the velocity information within $\pm 10^\circ$ longitude about both centres is ignored and only the velocity integrated emission is used to form the likelihood. The models are built iteratively, starting with a 2D disc model and then adding more complex features as necessary. The added features comprise: warping of the disc, a central bulge/bar, flaring in the outer Galaxy, and spiral arms. The warp and the flaring are significant only in the outer Galaxy and therefore do not have a large effect on the CO analysis that has only a small amount of gas in the outer Galaxy. The

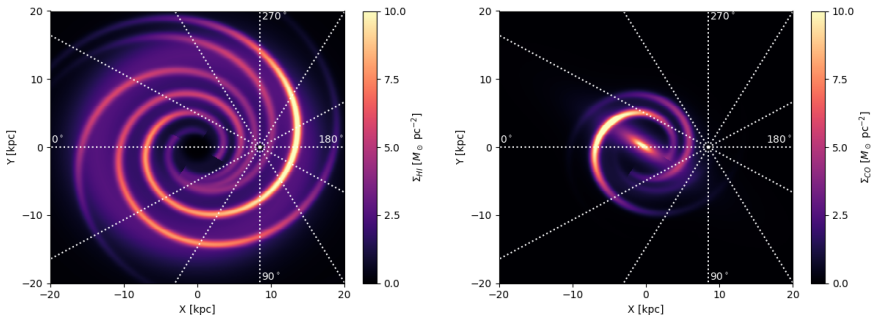

Figure 1: Surface density maps of the final models with H I on left and CO on right. The CO model is converted to surface density assuming $X_{CO} = 2 \cdot 10^{20}$ cm^{-2} K^{-1} (km/s)$^{-1}$. The sun is marked as a white point and the dashed lines show directions of longitudes at 30° intervals.

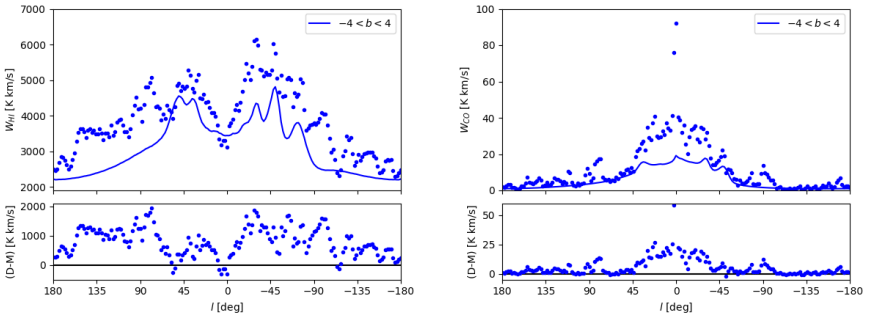

Figure 2: Longitude profile of the models (curves) overlaid on the data (points). The model and data are integrated over all velocity bins and averaged over the latitude range $-4° < b < 4°$. H I is on left and CO on right.

bulge/bar has only a small effect for the H I and the density ascribed to this component from the analysis is insignificant. Adding logarithmic spiral arms gives a significant improvement for both atomic and molecular gas models.

The surface density of the final distribution is shown in figure 1. The spiral arms are prominent in both H I and CO and the central bulge in CO. The model parameters were set such that the shape of the spiral arms are identical in both models, the radial density distribution is identical for the disk and spiral arms in each model but the relative contribution of each arm is free. For CO the density of one of the arms is effectively put to 0 and another is a factor $\sim$ 10 less dense than the densest arm and therefore barely visible in the figure. Comparison of the models to data is shown in the velocity integrated longitude profiles along the plane in figure 2. The model systematically under predicts the data which is to be expected when using the student-t likelihood that de-weights the tail of the residual distribution that is in this case dominated by positive residuals. This was by design so missing components would more easily show up as positive structures in the residuals. The spiral arm features are clearly visible in the model profiles as peaks and they match similar features in the data. The model chosen for this work is clearly not capable of reproducing all the complex features of the data even though the spiral arm structure reasonably matches that of the data.

3 Interstellar emission models

To demonstrate the effects these new gas distributions have on IEMs we incorporate them into the *GALPROP* code [14, 4]. The gas distributions in *GALPROP* are used for the calculation of energy losses and the production of secondary particles while the final γ-ray intensity maps are scaled such that the column density of each line of sight matches that estimated from the line surveys. The change in gas distributions therefore only affects the CR part of the IEM, the gas column density is corrected to match the observations. For simplification we only consider here a diffusive re-acceleration model with a homogeneous and isotropic diffusion with the CR sources distributed concentrated in spiral arms using the SA100 model from [4]. The CR source distribution is combined with the old 2D gas distributions from *GALPROP* and the new 3D gas distributions resulting in two new models. These models are compared to a model having the 2D CR source distribution SA0 and the old 2D gas distribution.

The CR propagation parameters are tuned to match observations of secondary CRs whose predictions depends on both the gas and CR source distribution. To have a consistent comparison, the propagation parameters of each of the 3 models is tuned to the same CR data. The new gas distributions have a large effect on the propagation parameters, reducing

the diffusion coefficient and the Alfvén speed by a factor of ~ 2. This is because the integrated column density of the new distributions around the location of the sun is smaller by about a factor of 2 resulting in less production of secondaries that is compensated for by having slower diffusion. The energy losses of the CRs are also affected and the estimated parameters for solar modulation and low energy CR injection are affected by the change in gas distribution.

The effect on the interstellar emission is illustrated in figure 3 that shows the ratio of the total γ-ray intensity of the models employing the SA100 CR source distribution to the reference model with the SA0 distribution. The 3D CR source distribution results in a doughnut like excess centred on the GC that is caused by a general increase in CR flux in the inner Galaxy combined with lack of CR sources near the GC. The reduced diffusion in the model with the new gas distribution results in a more confined excess around the plane and less emission in the outer Galaxy. The increased emission at low energies is a result of the change in modulation during the tuning of the propagation parameters.

GALPROP development is partially funded via NASA grants NNX13AC47G and NNX17AB48G. Some of the results in this paper have been derived using the HEALPix [12] package.

References

[1] Ackermann, M., et al. 2012, ApJ, 750, 3
[2] Ajello, M., et al. 2016, ApJ, 819, 44
[3] Johannesson, G., Moskalenko, I. V., & Porter, T. 2013, Br. J. of Phys., ICRC2013, 0913
[4] Porter, T. A., Johannesson, G., & Moskalenko, I. V. 2017, ArXiv e-prints
[5] Kissmann, R., Niederwanger, F., Reimer, O., & Strong, A. W. 2017, in American Institute of Physics Conference Series, Vol. 1792, 6th International Symposium on High Energy Gamma-Ray Astronomy, 070011
[6] Ferrière, K. M. 2001, Reviews of Modern Physics, 73, 1031
[7] Levine, E. S., Blitz, L., & Heiles, C. 2006, ApJ, 643, 881
[8] Pohl, M., Englmaier, P., & Bissantz, N. 2008, ApJ, 677, 283
[9] Nakanishi, H., & Sofue, Y. 2016, PASJ, 68, 5
[10] Kalberla, P. M. W., et al. 2005, A&A, 440, 775
[11] Dame, T. M., Hartmann, D., & Thaddeus, P. 2001, ApJ, 547, 792
[12] Górski, K. M., et al. 2005, ApJ, 622, 759
[13] Sofue, Y., Honma, M., & Omodaka, T. 2009, PASJ, 61, 227
[14] Vladimirov, A. E., et al. 2011, Computer Physics Communications, 182, 1156

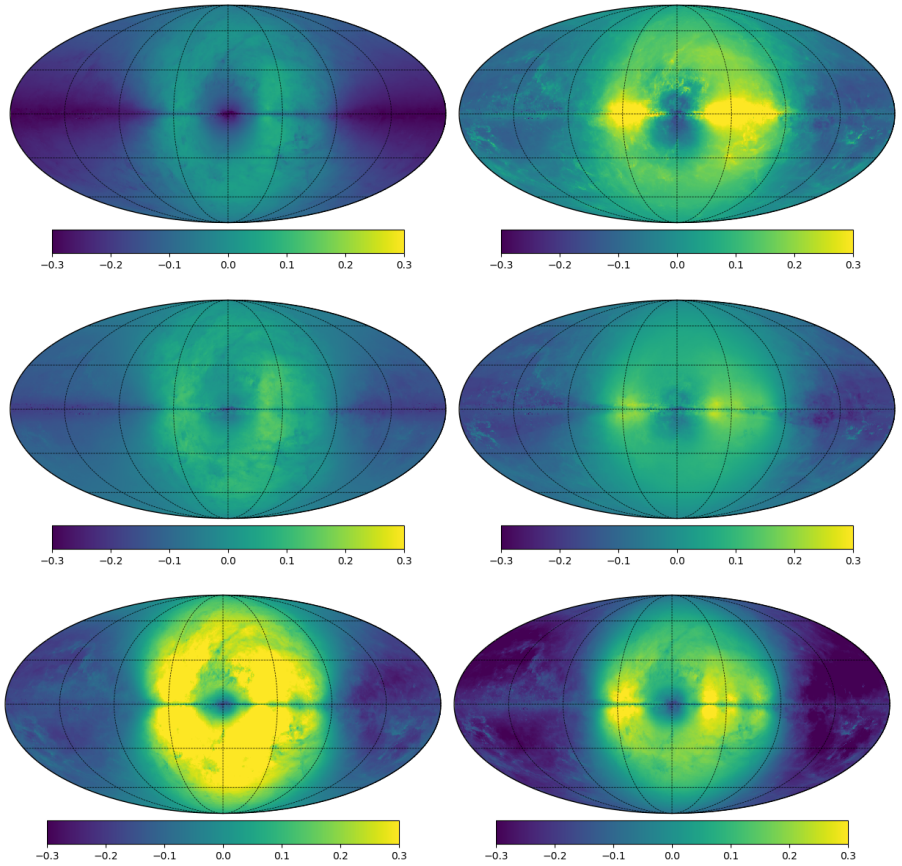

Figure 3: Fractional residuals for the total γ-ray intensity (π^0-decay, Bremsstrahlung, and IC) at 30 MeV, 1.0 GeV, and 100 GeV energies (top to bottom, respectively) for SA100-2D gas (left) and SA100-3D gas (right) compared to 2D CR and gas reference model. The maps are in Galactic coordinates with $l, b = 0°, 0°$ at the centre with l increasing to the left. The longitude meridians have 45° spacing and latitude parallels have 30° spacing.